Colloid Polym Sci 275:869–875 (1997)
© Steinkopff Verlag 1997

ORIGINAL CONTRIBUTION

Y.-K. Leong

Effects of steric and hydrophobic forces on the rheological properties of ZrO_2 suspensions

Received: 23 May 1997
Accepted: 4 June 1997

Y.-K. Leong[1]
Advanced Mineral Products
Research Centre
The University of Melbourne
Parkville 3052, Australia

[1]*Present address*:
Dr. Y.-K. Leong (✉)
Department of Chemistry
University of Malaya
50603 Kuala Lumpur, Malaysia

Abstract The effect of pH on the flow behavior of ZrO_2 suspensions containing polyacrylic and octanoic acids was evaluated. In the flocculated pH regime, the flow behavior is highly shearthinning and can be described by a power-law model. The shear-thinning behavior increases with increasing degree of flocculation. Maximum shearthinning was observed at the zero zeta potential condition. Hydrophobic interaction arising from adsorbed octanoic acid was found to enhance the shear-thinning behavior. No such enhancement was observed for adsorbed polyacrylic acid. It was also illustrated that the viscosity–pH behavior is a mirror image of the yield stress–pH behavior. A quantitative particle-pair interactions model incorporating steric and hydrophobic interactions was proposed to explain the effects of polyacrylic and octanoic acids on the maximum yield stress.

Key words Shearthinning behavior – yield stress – hydrophobic – steric – pH

Introduction

Polymeric dispersants and flocculants, and flotation agents or surfactants are often added to aqueous suspensions in order to achieve the desired properties for processing. These additives alter the surface properties of the particle through adsorption. Commercial dispersants are often highly charged low molecular weight anionic polyelectrolytes such as polyacrylates [1–4] and polyphosphates [5]. These additives, often in a salt form, impart a high surface charge upon adsorption. Addition of these (partially) neutralized polyelectrolytes increases the pH of the suspensions where their dispersing action is most effective. Polymeric flocculants are generally of high molecular weight. They can be ionic or nonionic. These additives bridge the particles creating large flocs. Bridging flocculation is most effective at low polymer concentrations or surface coverages. For a better understanding of polymer bridging in particulate system reference should be made to an review article by Dickinson and Ericksson [6]. Flotation agents are chemicals containing a hydrophilic head group and a hydrophobic tail such as surfactants.

The effect of dispersants on aqueous suspension rheology is a well-studied subject [1–4]. The main function of a dispersant is to reduce the viscosity of a suspension by transforming a net attractive interparticle interaction to a repulsive one. Dispersion is attributed to the well-understood charge stabilization mechanism. However, in the flocculated pH regime, the action of dispersants on the interparticle force is not well studied and understood. Only recently adsorbed dispersants were found to weaken the interparticle attractive force by steric interaction [5, 7]. The effect of polymer bridging on the suspension rheology has also been studied quite extensively by Otsubo et al. [8–10]. The floc structure formed by polymer bridging is usually irreproducible and changes continuously in a shear field. As a result, the rheological properties of bridged floc suspensions are not particularly reproducible. The effect of surfactants on suspension rheology is the least understood topic. A "new" and relatively large attractive force arising from adsorbed surfactants was recently measured between the mica sheets [11] and between particles in suspensions [12–14].

We [7, 15] reported the effect of polyacrylic acid (PAA) on the maximum yield stress, located at zero zeta potential, of colloidal ZrO_2 suspensions. The yield stress is a measure of the strength of the attractive interparticle force. PAA was found to reduce the maximum yield stress and the extent of reduction increases with increasing PAA concentration and with decreasing PAA molecular weight. This reduction was attributed to the formation of a steric barrier by the adsorbed PAA which keeps the interacting particles further apart. High molecular weight PAA is less effective because of polymer bridging.

The "new" attractive force arising from adsorbed surfactant which is commonly referred to as the hydrophobic force. It has a much larger magnitude and range than the van der Waals. As a result, adsorbed surfactant increases the maximum yield stress of ZrO_2 suspensions [12–14] by as much as sixfold [14]. The origin of the hydrophobic force is still a major topic of debate. This force has been variously attributed to entropic [16, 17] and hydrodynamic [18] effects, and interactions between charged patches [19].

In this study the flow and yield stress properties of flocculated ZrO_2 suspensions containing an adsorbed dispersant and surfactant are presented and discussed.

Materials and methods

The ZrO_2 powder, from Z-Tech (ICI Advanced Ceramics Australia), has a BET surface area of 15.1 m^2/g and an isoelectric point at pH 7.0 [5]. The particle size distribution based on number was measured with a LS130 Coulter Counter. It has a D_{90} of 0.282 μm, D_{50} of 0.148 μm and D_{10} of 0.106 μm (or D_{90} of 0.58 μm, D_{50} of 0.25 μm and D_{10} of 0.13 μm based on volume). The solid density of the ZrO_2 is approximately 5880 kg/m^3. The chemical additives used were PAA and octanoic acid. The PAA of molecular weight 2000 was supplied by Aldrich Chemical Co. The octanoic acid, $CH_3(CH_2)_6COOH$, was provided by Eastman Kodak Organic Chemicals.

The following procedure was adopted in the preparation of a ZrO_2 suspension with an additive. The polyacrylic or octanoic acid was dissolved first in a known amount of "Milli-Q" water at an alkaline pH. An appropriate amount of ZrO_2 was then added to the solution. The suspension was sonicated for a period of 1 min with a 0.75 in horn of a Branson B-30 sonifier. The sonifier was operated at 50–60% of the maximum power output of 350 W. The prepared suspension was allowed to rest for at least a day.

Concentrated nitric acid (1–15.8 M) was used to change the suspension pH so as to minimize the extent of dilution. Localized flocculation was observed to occur in the vicinity of the acid or alkaline droplets. These droplets were redispersed by sonication. After each pH change the suspension was rested for at least 2 h and then stirred vigorously with a spatula before conducting the yield stress measurement. The pH was measured with an Orion 720A pH meter. The flow behavior was determined using a cone-and-plate Bohlin viscometer and the yield stress was measured with a vane rheometer [20].

Results and discussion

The effect of PAA on the yield stress–pH behavior of a 57 wt% ZrO_2 suspension is shown in Fig. 1. The concentration of added PAA ranged 0.0–1.0 dwb% (gPAA/100 gZrO_2). Yield stress data for 0.0, 0.2, 0.5 and 1.0 dwb% PAA are given elsewhere [7]. The reduction in maximum yield stress by PAA has already been discussed in an earlier paper [7]. All suspensions have an average ionic strength of 0.05 M KNO_3 calculated based on the amount of KOH and HNO_3 added at the maximum yield stress.

Figure 1 shows the yield stress curve for no PAA is nearly an ideal parabola. Complete dispersion occurs at pH less than 5.0 and more than 10.0. The yield stress curve for PAA is less parabolic because of an apparent absence of a low pH dispersed region. Only at the lowest PAA concentration of 0.05 dwb% was a low-pH dispersed region observed. Even then, dispersion starts at a much lower pH of 3.0 despite both (compared with no PAA) having nearly the same pH of maximum yield stress.

Adsorbed PAA also shifts the start of the high-pH dispersed region to a lower pH. The degree of shift increases with PAA concentration. At 0.5 dwb% PAA complete dispersion starts at pH 5.5 where the underlying surface charge is positive. Adsorption of 0.5 dwb% PAA is sufficient to neutralize all the positive charges and with some negatively charged carboxylic group left over.

The absence of a low-pH dispersion region is attributed to two factors. Firstly, the carboxylate group does not transform into a positively charged species even at a very low pH level. Hence, adsorbed PAA does not enhance the positive surface charge of the ZrO_2. Secondly adsorbed PAA also reduces the concentration of positive charge sites. As a result, the ZrO_2 particles cannot acquire enough positive charges for complete dispersion at low pH levels except at very low PAA concentrations.

At high PAA concentrations, the ZrO_2 particle's surface property is governed by the surface property of the adsorbed PAA. As a result, the pH of zero zeta potential or

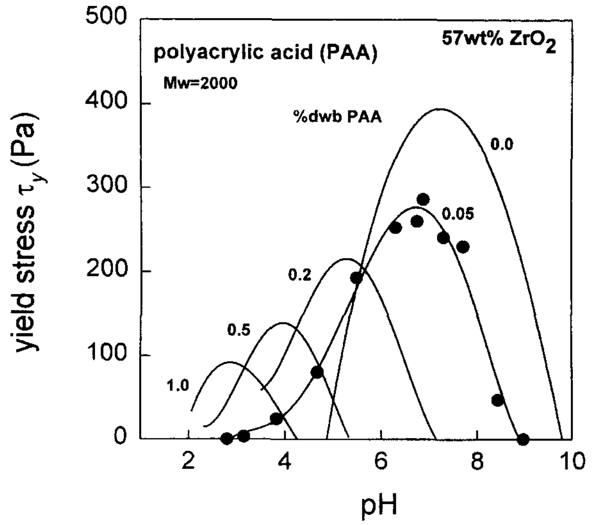

Fig. 1 Effect of polyacrylic acid on the yield stress–pH behavior of a 57 wt% ZrO_2 suspension

maximum yield stress approaches the apparent isoelectric point of carboxylate at pH 2.0 at high PAA concentrations. For example, the suspension with 1.0 dwb% PAA which has a monolayer surface coverage of 18 Å^2/acrylic acid unit (the monolayer coverage for a surfactant is 25 Å^2/molecule [21]), has a pH of maximum yield stress of 3.0.

Figure 2a shows a logarithmic plot of viscosity versus shear rate for a 57 wt% ZrO_2 suspension illustrating the effect of pH. Between pH 4.6 and 9.4, the flow behavior is highly shearthinning as indicated by a sharp decrease in viscosity with increasing shear rate. Like the maximum yield stress, the maximum viscosity (at any given shear rate) is located at pH 7.0. Figure 2b is a similar plot of viscosity versus shear rate for a 57 wt% ZrO_2 suspension containing 1.0 dwb% polyacrylate. A low molecular weight ammonium polyacrylate was used. At pH 7.5 and 6.8, the flow behavior is slightly shearthinning. The shearthinning behavior becomes increasingly more pronounced at lower pH levels. The viscosity is maximum at pH 3.0.

For both suspensions, the relationship between the log of viscosity and the log of shear rate is clearly linearly in the flocculated pH region. A power-law model,

$$\mu = K\dot{\gamma}^{n-1}\,, \tag{1}$$

therefore described the flow behavior where μ is the viscosity, K the consistency index and n the shear rate exponent. A low exponent value implies a very shearthinning fluid. The dependence of n on pH for suspensions with none and 1.0 dwb% polyacrylate is shown in Fig. 3. In both cases, n decreases with increasing yield stress or degree of flocculation. A minimum value was observed at the maximum yield stress, i.e. at pH 7.0 for no additive and 3.0 for

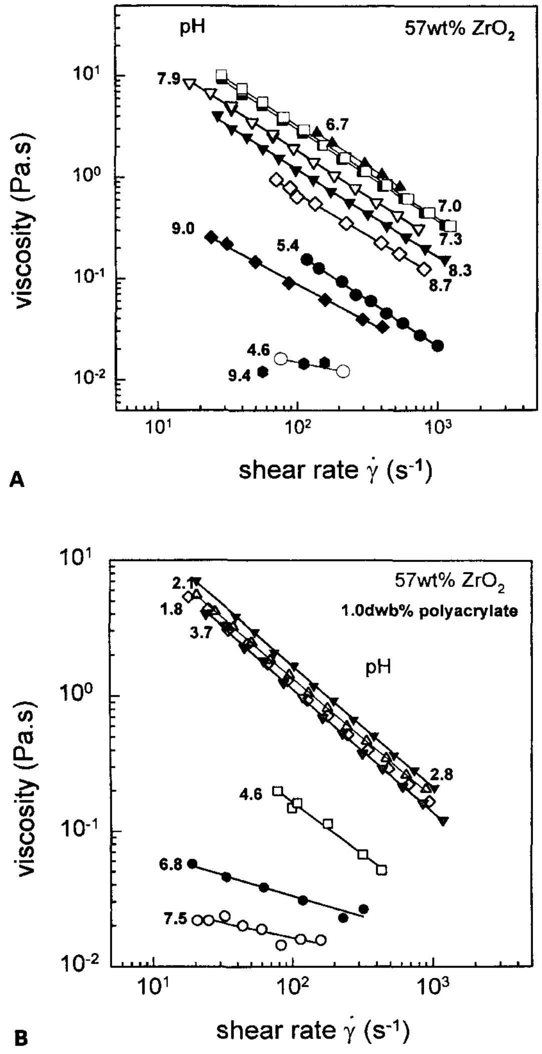

Fig. 2A Effect of pH on the viscosity–shear rate behavior of a 57 wt% ZrO_2; **B** Effect of pH on the viscosity–shear rate behavior of a 57 wt% ZrO_2 suspension containing 1.0 dwb% polyacrylate

1.0 dwb% polyacrylate. However, there is no significant difference between the two minima.

The effect of 0.1 dwb% octanoic acid on the yield stress–pH behavior of a 41.5 wt% ZrO_2 suspension is shown in Fig. 4. Data for no additive were also presented. Octanoic acid clearly increases the maximum yield stress from 100 to 170 Pa. A clear indication that octanoic acid adsorption has taken placed is the shift of the pH of maximum yield stress to a lower value. At 0.1 dwb% octanoic acid, the maximum yield stress is located at pH 6.0 which is also the pH of zero zeta potential [14].

The viscosity–shear rate data for a 41.6 wt% (0.11 volume fraction) ZrO_2 suspension obtained at various fixed pH levels are shown in Fig. 5a. Newtonian flow

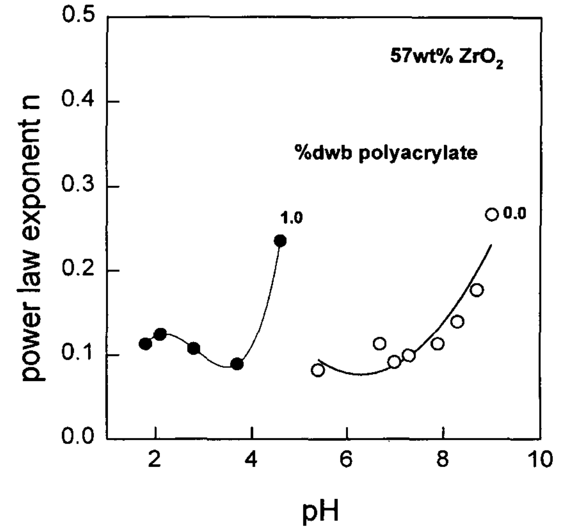

Fig. 3 Plot of shear rate exponent versus pH for a 57 wt% ZrO_2 suspension. Open circle: no polyacrylic acid; Full circle: 1.0 dwb% polyacrylic acid

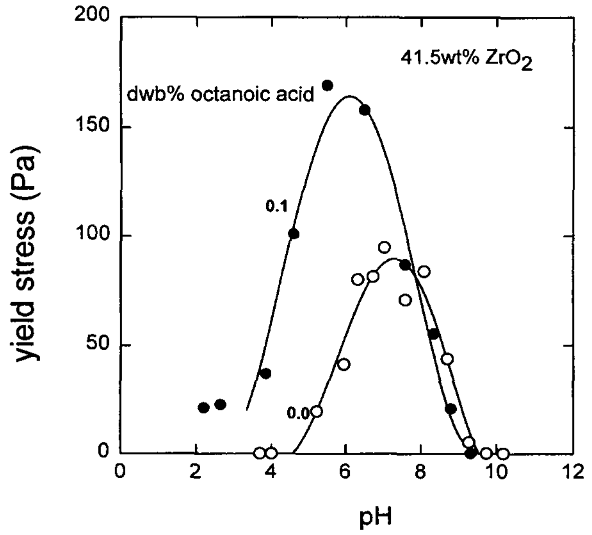

Fig. 4 Plot of yield stress versus pH for 41.5 wt% ZrO_2 suspension. Open circle: no octanoic acid; Full circle: 0.1 dwb% octanoic acid

behavior was observed at pH more than 10.0 and less than 4.0. The suspension displays a very pronounced shear-thinning behavior at pH between 5.2 and 9.3. The logarithmic decrease in viscosity with shear rate is highly linear and hence can be described by the power-law model.

The viscosity–shear rate data for a 41.4 wt% ZrO_2 suspension containing 0.1 dwb% octanoic acid are shown in Fig. 5b. The suspension displays Newtonian behavior at pH 9.3 and very shearthinning behavior at pH 8.8 and less. Again the power-law model describes the flow behavior adequately in the flocculated pH regime.

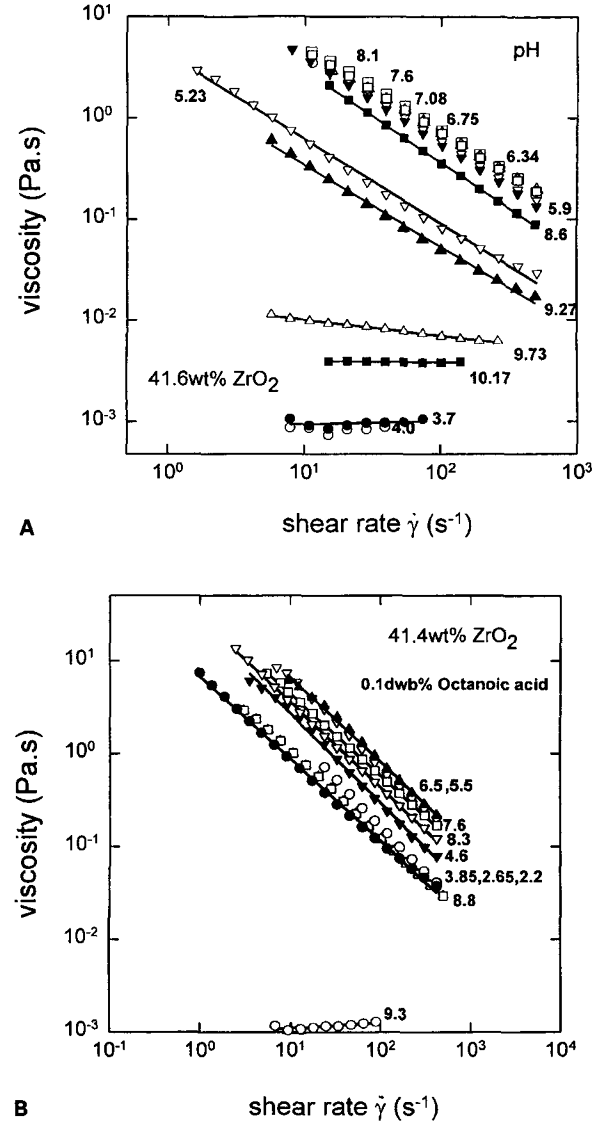

Fig. 5A Effect of pH on the viscosity–shear rate behavior for a 41.6 wt% ZrO_2 suspension; **B** Effect of pH on the viscosity–shear rate behavior for a 41.4 wt% ZrO_2 suspension containing 0.1 dwb% octanoic acid

The high-pH dispersed region occurs at a lower pH of 9.3 for the suspension with 0.1 dwb% octanoic acid. This is due to octanoic acid adsorption at pH above 9.3. Like PAA, adsorbed octanoic acid increases the total negative charge on the ZrO_2 particles. The low-pH dispersed region is however absent even at pH as low as 2.2. There are two reasons. Firstly, the adsorbed octanoic acid does not increase the total positive charge. And secondly the strong hydrophobic attractive force extending over several hundred nanometers [22, 23] ensured attraction at large interparticle separation. In contrast, the suspension with no octanoic acid is already dispersed at pH 4.0.

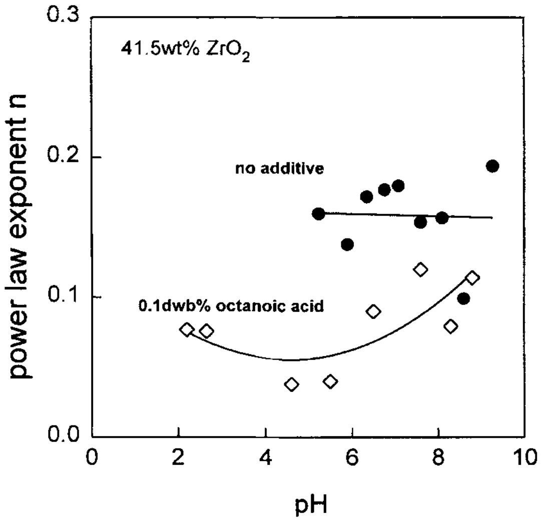

Fig. 6 Plot of shear rate exponent versus pH for a 41.5 wt% ZrO_2 suspension. Full circle; no octanoic acid; Open diamond: 0.1 dwb% octanoic acid

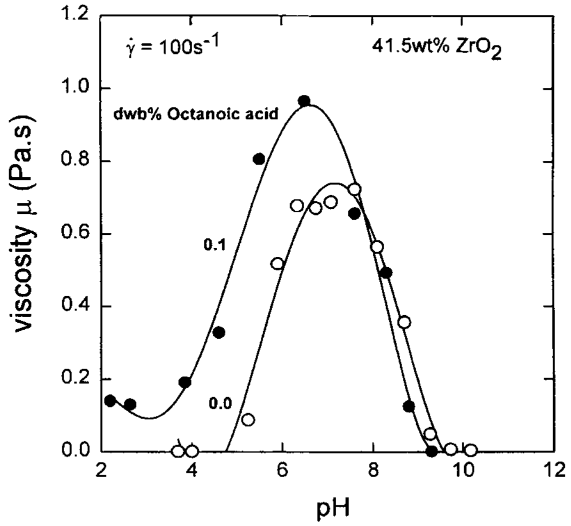

Fig. 7 Plot of viscosity versus pH for a 41.5 wt% ZrO_2 suspension. Open circle: no octanoic acid; Full circle: 0.1 dwb% octanoic acid

The dependence of shear rate exponent on pH for none and 0.1 dwb% octanoic acid is shown in Fig. 6. The exponent for octanoic acid is consistently smaller. The value falls in the range of between 0.05 and 0.12. With no octanoic acid the value is between 0.15 and 0.21. Octanoic acid, therefore, enhances the shearthinning characteristics of the suspension. A minimum value was observed at pH between 4.0 and 6.0 for 0.1 dwb% octanoic acid where the suspension is most flocculated. For no octanoic acid, the exact location of the pH of the minimum exponent is less obvious as the data were too erratic. Only a linear relationship can be drawn. The minimum has been shown for a higher ZrO_2 concentration to occur at pH 7.0 (see Fig. 3).

A comparison of the viscosity-pH plot for the two suspensions is shown in Fig. 7. The viscosity was evaluated at a shear rate of $100\,s^{-1}$. The viscosity–pH curve is almost a mirror image of the yield stress–pH. The maximum viscosity is 43% larger in the presence of octanoic acid. It is 1.0 Pa s compared with 0.7 Pa s for no octanoic acid. However, the maximum yield stress increase was 70%.

There are three forces of interaction between a ZrO_2 particle pair containing adsorbed polyacrylic acid. These are the van der Waals, steric and electrostatic. With octanoic acid there is an additional force, the hydrophobic. The total interaction energy V_T is assumed equal to the sum of the energy of each force component:

$$V_T = V_{\mathrm{vdw}} + V_{\mathrm{elec}} + V_{\mathrm{steric}} + V_{\mathrm{hp}} \,, \qquad (2)$$

where V_{vdw} is the van der Waals, V_{elec} the electrostatic, V_{steric} the steric component and V_{hp} the hydrophobic force component. The well-known expression for the van der Waals interaction energy is

$$V_{\mathrm{vdw}} = -\frac{RA}{12H} \,, \qquad (3)$$

where R is the particle radius, A the effective Hamaker constant and H the surface-to-surface separation. For electrostatic interaction energy it is

$$V_R = 2\pi R \varepsilon \varepsilon_0 \psi_0^2 \mathrm{e}^{-\kappa H} \,, \qquad (4)$$

where ψ_0 the surface potential, ε_0 the permittivity in free space and ε the relative permittivity of the medium. Eq. 4 is only valid for low surface potential, $\psi_0 < 50$ mV [17]. As the hydrophobic force is made up of a short and a long-range component [22, 23], the interaction energy can be represented by

$$V_{\mathrm{hp}} = -\left[C_1 \mathrm{e}^{-H/\lambda_1} + C_2 \mathrm{e}^{-H/\lambda_2}\right] , \qquad (5)$$

where C_1 and C_2 are the constants, and λ_1 and λ_2 are the characteristic decay length of the short- and long-range components respectively. λ_1 and λ_2 are of the order of 25 and 250 Å, respectively. The expression often assumed for V_{steric} is

$$V_{\mathrm{steric}} = \frac{K}{H^m} \,, \qquad (6)$$

where K is a constant and m the exponent. The value of m ranges from 3.4 for particle with grafted polymer of different chain length [24] to 20 for a PMMA microgel

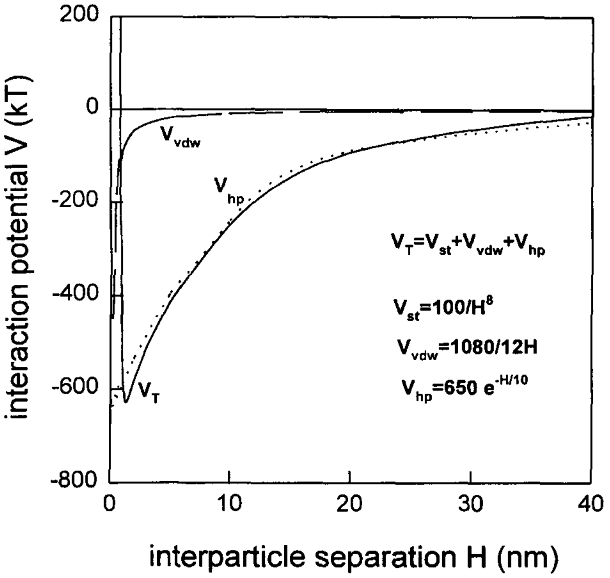

Fig. 8 Total and individual component interaction energy as a function of interparticle separation

spheres [25]. Values of K and m were chosen such that V_{steric} is infinite when the adsorbed layers on the interacting particles are touching. This energy should decrease rapidly to zero once particle–particle contact is lost.

Figure 8 shows a plot of the total interaction energy V_T ($= V_{vdw} + V_{\text{stenc}} + V_{hp}$) versus interparticle separation H at zero zeta potential condition. It is a qualitative description of particle pair interaction in the suspension containing 0.1 dwb% octanoic acid at the maximum yield stress or viscosity. V_{vdw} and V_{hp} were also plotted for comparison. All essential features of steric, van der Waals and hydrophobic interaction energies are clearly shown. For V_{steric} purely empirical values were chosen for the two constants K and m such that a steric barrier thickness of 0.6 nm (assumed to represent the thickness of adsorbed octanoic acid layer) was obtained. More realistic values for the particle size (74 nm = number-average radius) and effective Hamaker constant (6.0×10^{-20} J) were used to calculate V_{vdw}. We used the result of Israelachvili and Pashley [11], where one exponential term was used to describe the hydrophobic interaction potential V_{hp}. A realistic decay length of 10 nm was used and the constant C was chosen such that as H approaches the minimum separation of 0.3 nm [5] for no adsorbed additive, V_{hp} is about twice V_{vdw}, i.e. similar to the maximum yield stress ratio with and without 0.1 dwb% octanoic acid of 1.7. A hard-wall steric repulsion is clearly seen at $H < 12$ Å in Fig. 8. At $H > 12$ Å, the steric repulsive energy becomes unimportant. Another feature shows the magnitude of V_{hp} being larger than V_{vdw} at $H > 0.3$ nm.

In the absence of an adsorbing additives, only the van der Waals interaction energy needs to be overcome to breakdown the network structure. The van der Waals energy is about 325 kT at the minimum separation of $H = 0.3$ nm [5, 26]. With octanoic acid V_T shows a deeper energy well of about 600 kT at $H = 1.2$ nm because of the additional hydrophobic interaction potential. This deeper energy well represents the larger yield stress and viscosity obtained in the presence of octanoic acid. The lower yield stress and viscosity obtained in the presence of PAA is also represented by the result in Fig. 8. Adsorbed PAA at 1 dwb% produced a steric barrier thickness of 0.5 nm [5, 7], i.e. $H = 1.0$ nm. From the van der Waals energy curve, the interaction energy is only 90 kT at $H = 1.0$ nm.

Conclusions

The shearthinning behavior increases with increasing degree of flocculation. Hydrophobic forces enhance the shearthinning behavior of ZrO_2 suspensions. No enhancement was observed with steric forces.

Acknowledgment I am grateful to the Australia Research Council for supporting this work through a Special Research Centre Grant.

References

1. Bleier A, Westmoreland CG (1988) In: Attia YA, Moudgil BM, Chander S (eds) Interfacial Phenomena in Biotechnology and Materials Processing. Elsevier, Amsterdam, pp 217–236
2. Cesarano III J, Aksay IA (1988) J Amer Ceram Soc 71:1062–1067
3. Leong YK, Boger DV (1991) Ceram Trans 19:83–90
4. Heijman SGJ, Stein HN (1995) Langmuir 11:422–427
5. Leong YK, Scales PJ, Healy TW, Boger DV, Buscall R (1993) J Chem Soc Faraday Trans 89:2473–2478
6. Dickinson E, Eriksson L (1991) Adv Colloid Interface Sci 34:1–29
7. Leong YK, Scales PJ, Healy TW, Boger DV (1995) Colloids Surf A Physicochem Eng Aspects 95:43–52
8. Otsubo Y, Watanabe K (1989) J Colloid Interface Sci 133:491–496
9. Otsubo Y, Watanabe K (1990) Colloids Surf 50:341–352
10. Otsubo Y (1990) Langmuir 6:114–118
11. Israelachvili JN, Pashley RM (1984) J Colloid Interface Sci 98:500–514
12. Leong YK (1994) Mater Des 15:141–147
13. Leong YK, Boger DV, Scales PJ, Healy TW, Buscall R (1993) J Chem Soc Chem Commun 639–641

14. Leong YK, Boger DV, Scales PJ, Healy TW (1996) J Colloid Interface Sci 181:605–612
15. Leong YK, Healy TW, Boger DV (1993) In: Adair JH, Casey JA, Venigalla S (eds) Handbook on Characterisation Techniques for Solid-Solution Interface. The Amer Ceram Soc, pp 255–269
16. Israelachvili JN, Kott SJ, Gee ML, Witten TA (1989) Langmuir 5:1111–1115
17. Israelachvili JN (1992) Intermolecular & Sulface Forces. Academic Press, London
18. Ruckenstein E, Churaev N (1991) J Colloid Interface Sci 147:535–538
19. Miklavic SJ, Chan DYC, White LR, Healy TW (1994) J Phys Chem 98: 9022–9032
20. Nguyen QD, Boger DV (1983) J Rheol 27:321–349
21. Wakamatsu T, Fuerstenau DW (1968) Adv Chem Ser 79:161–172
22. Tsao YH, Yang SX, Fannell ED, Wannerström H (1991) Langmuir 7:3154–3159
23. Tsao YH, Fannell ED, Wennerström H (1993) Langmuir 9:779–785
24. D'Haene P (1992) PhD Dissertation, Katholieke Universiteit Leuven, Belgium
25. Ackerson BJ, Paulin SE (1994) 8th Int Conf Surf Colloid Sci. Abstracts, Adelaide, pp 190
26. Leong YK (1996) Colloids Surf A Physicochem Eng Aspects 118:107–114